Physics – Uspekhi **55** (7) 700 – 708 (2012)

METHODOLOGICAL NOTES PACS numbers: 01.50.Pa, 41.20.Cv, **45.50.–j**

Electrostatic oscillators

V A Saranin

DOI: 10.3367/UFNe.0182.201207e.0749

Contents

Abstract. Several types of electrostatic oscillators, with an electrically charged ball as the load, are examined, noting that a physical and a mathematical electrostatic pendulum together with a grounded conducting plate form a bistable oscillator for which the same set of parameters produces two stable and one unstable equilibrium positions. For this oscillator, bifurcation curves are drawn and nonlinear oscillations are studied. The electrostatic string pendulum also has a bifurcation point and, besides, can self-oscillate when electrically broken down. It is shown that a liquid–liquid interface placed in an external electric field can be regarded as an electrostatic oscillator. Experimental results confirming theoretical predictions are presented.

1. Introduction

In this paper, we use the term "electrostatic pendulum" to refer to a physical pendulum modified such that its ball is charged. This kind of pendulum has been used, in particular, as an electrostatic dynamometer to measure the electrostatic force [1]. Experiments using such a dynamometer to measure the electric image force acting on a charge from a grounded conducting plate have shown that the electrostatic pendulum exhibits interesting properties under these conditions. In particular, there are bifurcation points in the working range of oscillator parameters that separate regions with stable equilibria, those with unstable equilibria, and those with neither of the two. Importantly, for one and the same set of pendulum parameters, the pendulum can simultaneously have one unstable equilibrium and two stable equilibria, which places it into the category of bistable Chua oscillators [2, 3], devices that exhibit chaotic behavior under certain conditions [2–4]. However, the electrostatic pendulum has a two-dimensional phase space, and therefore bistability cannot drive it to chaotic behavior. Bifurcation properties also occur in the string electrostatic pendulum. Under certain conditions, systems containing such a pendulum exhibit self-oscillations. Another example of where such self-oscillations are observed is given by distributed oscillatory systems (capillary devices, etc.).

Based on the results obtained, electrostatic oscillators are arguably physical objects of considerable scientific and methodological interest.

V A Saranin Korolenko Glazov State Pedagogical Institute, ul. Pervomaiskaya 25, 427621 Glazov, Udmurt Republic, Russian Federation
Tel. 7 (34141) 558 57
E-mail: saranin@ggpi.org, val-sar@yandex.ru

Received 14 January 2011, revised 12 October 2011
Uspekhi Fizicheskikh Nauk **182** (7) 749 – 758 (2012)
DOI: 10.3367/UFNr.0182.201207e.0749
Translated by E G Strel'chenko; edited by A M Semikhatov

2. Electrical image method in experiment

The correct way to explain the electrical image method is by modeling the conductor as a half-space bounded by a planar surface [5]. Then, if the field-producing charge q is positive, $q > 0$, the surface acquires an excess negative charge, whereas the corresponding positive charge is at infinity and has no effect on the situation. We then have the full image of the charge, $q' = -q$, placed at the same distance from the surface as the source. As a consequence, the source charge is subject to the Coulomb force from the image charge, which attracts the charge to the plane and is given by $F = kq^2/4S^2$ (assuming the charge is point-like), where S is the distance between the charge and the plane.

A frequently used approach, however (see, e.g., Refs [6, 7]), is to consider a large, thin, grounded conducting plate instead of a conducting half-space, in which case the full imaging of the charge is assumed. This assumption was tested experimentally using an electrostatic dynamometer [1] and a grounded duralumin plate $645 \times 380 \times 2$ mm^3 in size. A foam plastic ball 24 mm in diameter coated with thin aluminum foil was glued to a ballpoint pen rod with a wire from a high-voltage source passing inside. The Coulomb force can cause the entire system to rotate (Fig. 1a). The remaining setup parameters are as follows: $a = \mathrm{OC} = 2.0$ mm, $b = 60$ mm, $h = 100$ mm, and $m = 1.1$ g. A voltage of 15 kV was applied to the ball from a high-voltage source through an insulated lead. Suspending

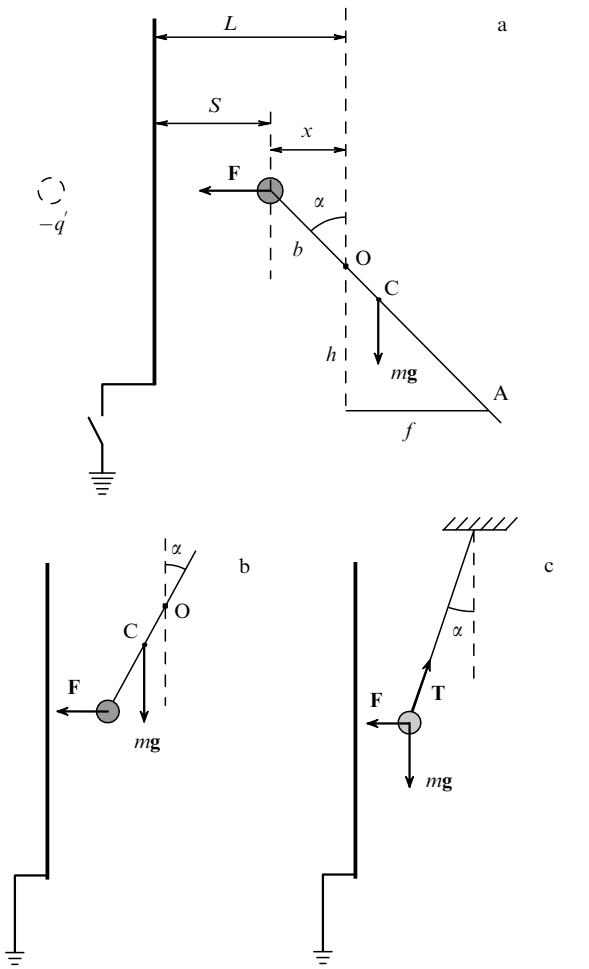

Figure 1. (a) Schematic of the electrostatic dynamometer. Point C is the center of mass. The rotation axis passes through point O. (b, c) Possible varieties of the electrostatic pendulum.

the plate by a fishing line eliminated such factors as the surface conductivity of the surrounding bodies and the additional induced capacitance, thereby insulating the plate from all bodies except the grounding wire.

When the pendulum is in its equilibrium position, the moment of the Coulomb force about the O axis is balanced by the moment of the entire system force of gravity,

$$Fb\cos\alpha = mga\sin\alpha\,, \tag{1}$$

or

$$F = \left(\frac{mga}{b}\right)\tan\alpha\,, \quad \tan\alpha = \frac{f}{h}\,, \quad F = \left(\frac{mga}{bh}\right) f\,. \tag{2}$$

Assuming the ball to be a point-like charge, the Coulomb force acting on it from the full image is

$$F = \frac{kq^2}{4S^2}\,, \quad k = \frac{1}{4\pi\varepsilon_0}\,, \tag{3}$$

where ε_0 is the electrodynamic constant. The distances L, b, h, and f (Fig. 1a) were measured by a millimeter ruler, and the distance S was calculated from

$$S = L - x = L - \frac{bf}{\sqrt{h^2 + f^2}}\,. \tag{4}$$

Based on experimental data, the force F was plotted (see Fig. 2) as a function of the inverse square of the ball-center–plate distance (each data point represents at least five measurements and the force is measured in relative units: in fact, the vertical axis is in centimeters because all the remaining quantities in the right-hand side of the last equation in (2) are constant). The straight line in the figure corresponds to the Coulomb law. For each initial ball position shown ($L = 8.0$, 8.2, 8.3 cm), there are two corresponding stable equilibrium positions of the pendulum, on the left and on the right from the shaded region. In this region, there are (according to theory) no stable equilibria for the pendulum, nor has experiment revealed any.

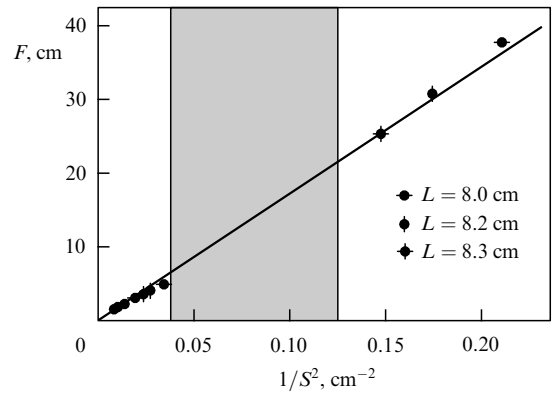

Figure 2. Interaction force between a charged ball and a grounded conducting plate as a function of the inverse square of the distance between the ball center and the plate. The straight line is the Coulomb law. In the shaded region, there are no stable equilibrium positions for the pendulum.

The experimental results obtained suggest that in a sufficiently large grounded conducting plane, the full charge image $q' = -q$ forms and that in the parameter range studied, the charge–source interaction force obeys the Coulomb law, as indeed it should. A quite unexpected finding was that the conducting plate–electrostatic pendulum system has the bistability property, i.e., can have two stable equilibria simultaneously for the same set of parameters.

3. Equilibrium and stability of an electrostatic pendulum

It is easy to see that the problem of the equilibrium of the pendulum in Fig. 1a is equivalent to the problems in Fig. 1b and Fig. 1c: the equilibrium condition for the pendulum in Fig. 1b is identical to Eqns (1) and (2), and that for the pendulum in Fig. 1c has the form $F/(mg) = \tan\alpha$ and can be reduced to Eqn (2) by renormalizing the constants m or g.

Using Fig. 1a, we obtain the dimensionless form of the equilibrium equation

$$Q^2 = (\widetilde{L} - \sin\alpha)^2 \tan\alpha\,, \quad Q^2 = \frac{kq^2}{4mgab}\,, \quad \widetilde{L} = \frac{L}{b}\,. \tag{5}$$

Transcendent equation (5) serves to determine the angular displacement of the pendulum from equilibrium as a function of two parameters, Q^2 and L. Because algebraic equations are easier to deal with, we eliminate the angle using the equality $\sin\alpha = \widetilde{L} - \widetilde{S}$, where $\widetilde{S} = S/b$. The tilde is omitted henceforth. The equilibrium condition then becomes

$$Q^2 = \frac{S^2(L - S)}{\sqrt{1 - (L - S)^2}}\,. \tag{6}$$

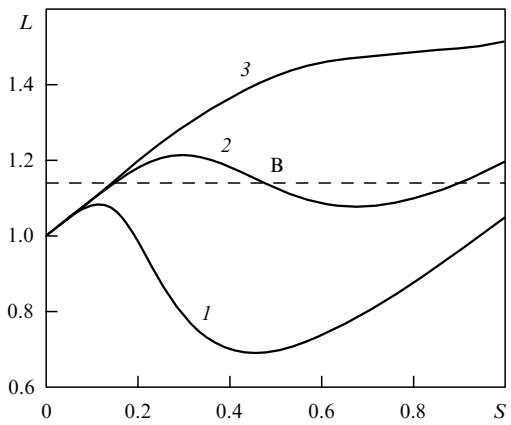

Figure 3. The distance S from the center of the ball in the equilibrium position to the plane as a function of the initial distance L for different values of the dimensionless ball charge Q.

Equation (6) determines S as a function of two parameters, L and Q^2. Equation (6) is difficult or impossible to solve for S analytically, but it allows, for example, expressing L explicitly as a function of S, with Q left as a parameter. After some algebra, we find that

$$L = S + \frac{Q^2}{\sqrt{S^4 + Q^4}} \,. \tag{7}$$

Figure 3 presents the inverse dependence $S(L)$ calculated for different values of Q. Curves *1*, *2*, *3* correspond to $Q^2 = 0.05$, 0.20, 0.60. For a given value of L on curve *2*, there are three values of S that correspond to the equilibrium equation. However, point B cannot be a stable equilibrium because decreasing L here corresponds to increasing S, which is physically impossible.

We see that curves *1* and *2* have local extrema, but curve *3* does not. To find what parameter values produce extrema, we take the derivative of L with respect to S and set it to zero to obtain

$$S^4 - 2^{2/3} Q^{4/3} S^2 + Q^4 = 0 \,. \tag{8}$$

Equation (8) has positive roots

$$S_{1,2} = \left[\frac{Q^{4/3}}{2^{1/3}} \pm \sqrt{\frac{Q^{8/3}}{2^{2/3}} - Q^4} \right]^{1/2} , \tag{9}$$

which exist only if

$$Q^2 \leqslant Q^2_{\max} = 0.5 \,. \tag{10}$$

This is indeed seen in Fig. 3: curve *3* corresponding to $Q^2 = 0.6$ has no extrema.

We find the conditions necessary for a pendulum initially positioned at $L \leqslant 1$ to have equilibria. From Eqn (7), setting $L = 1$ and replacing the equality sign by $\leqslant$, we find after some simple manipulation that

$$Q^2 \leqslant \frac{(1 - S)\, S^2}{\sqrt{S(2 - S)}} \,.$$

Analysis shows that the right-hand side of this equation has a maximum. To find it, we take the derivative and perform some algebra to obtain the quadratic equation

$$S^2 - 3S + \frac{3}{2} = 0 \,,$$

which has the suitable ($S < 1$) root

$$S = 1.5 - \sqrt{0.75} \approx 0.634 \,.$$

The corresponding maximum value is then given by $Q_1^2 \approx 0.158$. Hence, for $Q^2 > 0.158$ and $L < 1$, there can be no equilibria for the pendulum, which, accordingly, overturns on the plane.

The potential energy of a pendulum deviated from its original vertical position (in which the potential energy is taken to be zero) can be written as

$$W(x) = mga \left[\left(1 - \sqrt{1 - x^2} \right) + Q^2 \left(\frac{1}{L} - \frac{1}{L - x} \right) \right] , \qquad x = L - S = \sin\alpha \,. \tag{11}$$

In what follows, it is more convenient to directly use the displacement x of the ball from its initial position instead of S. Figure 4 shows the potential energy plotted in units of mga as a function of the deviation x of the pendulum from its equilibrium position. Corresponding to curves *1*, *2*, *3* are the initial positions $L < 1$: $L = 0.83$, 0.88, 0.90 and $Q^2 = 0.063$, 0.110, 0.220. We see that curve *1* has two local extrema, one for a stable and the other for an unstable equilibrium. Curves *2* and *3* do not contain equilibrium points, that is, the ball moves from its initial position straightaway to a position where it is in contact with the plane. Curves *4*, *5*, *6* correspond to initial position $L > 1$: $L = 1.27$, 1.29, 1.50, with $Q^2 = 0.29$, 0.34, 0.56. Importantly, curves *4* and *5* each have two local minima corresponding to stable equilibria and one maximum corresponding to an unstable equilibrium. Curve *6*, which corresponds to $Q^2 = 0.56 > 0.5$, contains only one stable equilibrium.

Further examination of the positions of extrema on the potential energy curves gave the following results. In Fig. 5, curve *1* corresponds to a set of parameters for which the maximum of the potential energy is zero, $\max W = 0$. The shaded area in Fig. 5a represents a range of parameters in which the pendulum has no stable equilibria and flips back from its equilibrium position, i.e., jumps to the position $x = L$ (contact with the plane) at $L \leqslant 1$. Curve *2* in Fig. 5a

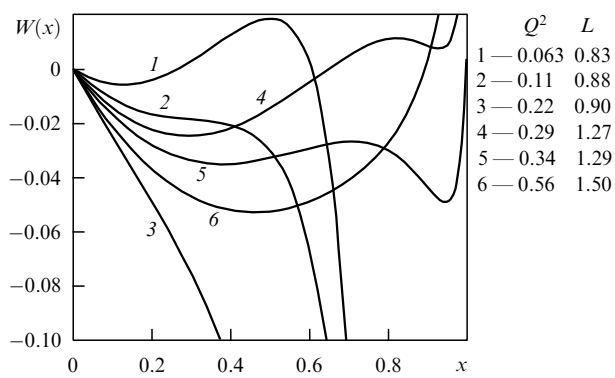

Figure 4. Potential energy of a pendulum as a function of the displacement of its center from the initial position (in dimensionless units) for different values of the control parameters L and Q.

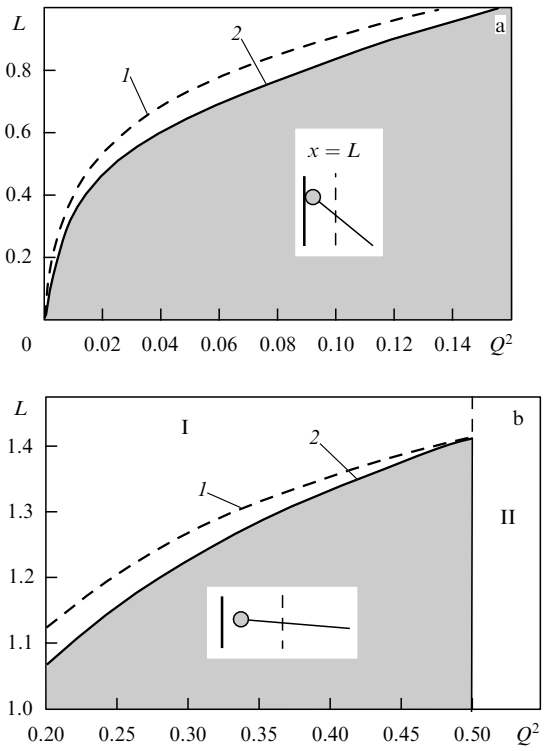

Figure 5. Curve *1* corresponds to the set of parameters for which the potential energy of the pendulum at the maximum drops to zero. Curve *2* in panel a is a bifurcation line that separates the region of parameters that contains a stable equilibrium from the (dashed) region that does not. Points on curve *2* in panel b are those where the first minimum of the potential energy curves disappears.

is in fact a bifurcation line separating the region that contains a stable equilibrium (unshaded region) from the region that does not (shaded region). Curves *1* and *2* in Fig. 5b have the same meaning; in the shaded region, however, there is now one stable equilibrium corresponding to the second minimum, in which $x \approx 1$. The bifurcation value of the parameter $Q^2_{\max} = 0.5$ separates regions II and I in Fig. 5b, with the former containing two stable equilibria and the latter only one.

Figure 6 presents a (Q^2, x) diagram of the stable and unstable equilibrium positions of the pendulum. In the shaded region, there are no stable equilibria, and given the appropriate value of L, the pendulum can flip back onto the plane to occupy the position $x = L$. The transition marked *1* corresponds to the transition to a stable equilibrium on curve *1* (see Fig. 4); *2* corresponds to the parameters of curve *2* in Fig. 4 and to the exit of the ball to the plane; *3* corresponds to the parameters of curve *3* in Fig. 4; *4* corresponds to the transition to the stable position of the first minimum of curve *4* in Fig. 4; *5* corresponds to the transition to the stable position of the second minimum on curve *5* in Fig. 4; *6* corresponds to the transition to the minimum on curve *6* in Fig. 4.

Experiments on the detection of stable equilibria of a pendulum used the electrostatic dynamometer circuit shown in Fig. 1a. The setup parameters were $a = 2.0$ mm, $b = 60$ mm, $h = 100$ mm, and $m = 1.1$ g. The experimental points are plotted in Fig. 6. The parameter $x = \sin\alpha$ was determined either from a computer photo image (at angles close to 90°) or as $\sin\alpha = f/\sqrt{f^2 + h^2}$. The parameter Q^2 was

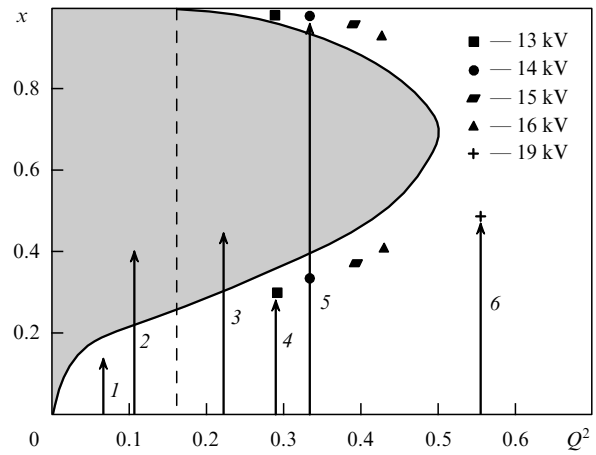

Figure 6. Map of the stable equilibria of the pendulum (bright region). The shaded region contains no stable equilibria. Different symbols refer to stable equilibria observed in experiments for different voltages.

calculated by the formula

$$Q^2 = \frac{f}{b^2 h}\left(L - \frac{fb}{\sqrt{f^2 + h^2}}\right)^2,$$

which follows from Eqns (1)–(3). We note that friction in the experiments was so strong that in each run, the pendulum first reached the first minimum and then, slightly pushed by a glass rod, made a transition to the equilibrium position corresponding to the second minimum. (This suggests that most of the friction force is due to air resistance to the motion of the pendulum.) These two equilibrium positions, the first and the second maxima, are shown in Figs 7a and 7b (the voltage is 15 kV). Comparisons of experimental results with theoretical predictions show not only obvious qualitative but also quantitative agreement: for example, according to theory, the minimum on curve *6* corresponds to $x \approx 0.48$, and the same value of x is obtained in experiment corresponding to transition *6* in Fig. 6.

It is now appropriate to ask at what distance the finite size of the ball has to be taken into account. It was shown in [8] that a charged ball and a finite conducting plane interact similarly to how two identical oppositely charged balls interact. A calculation predicts [8] that even at the center-to-center distance $l = 2.6R$ (R being the ball radius), the interaction energy of such balls is less than 10% greater than the Coulomb energy (with point-like charges located at

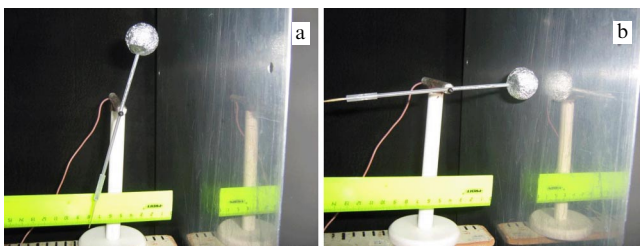

Figure 7. Photographs of two stable equilibrium positions of the pendulum that occur for the same set of parameters.

the centers of the balls). The rightmost minimum on curve *5* (Fig. 4) occurs at $x \approx 0.975$, meaning that the corresponding center-to-center distance between the ball and its image is $l = 2Sb = 2(L - x)\,b \approx 40.3$ mm, or $l \approx 3.36R$. Thus, because their interaction force differs from (exceeds) the Coulomb force only at very small distances between the ball and the plane, it follows that we are quite justified in adopting the point-like charge approximation.

Reference [9], a popular undergraduate problem solving book with eight editions published, poses the following problem: "A large metallic plate lies in the vertical plane and is connected to the ground. At the distance $a = 10$ cm from the plate there is a fixed point, from which a small ball of mass $m = 0.1$ g is suspended by a string of length $l = 12$ cm. When a charge q is delivered, the ball is attracted to the plate, resulting in the string deviating by the angle $\alpha = 30°$ from the vertical. Find the charge of the ball." The solution is given as

$$q = 2(a - l\sin\alpha)\,\sqrt{4\pi\varepsilon_0 mg\tan\alpha} = 20 \text{ nC}, \tag{12}$$

which easily follows from equating the projections of all the forces acting on the ball to zero. Exactly the same problem is considered in Refs [10, 11]. Neither the conditions of the problem nor the solution are correct, however. Indeed, the parameter L in this problem is $L = a/l \approx 0.83 < 1$, and the value of x corresponding to the angle of 30° is $x = \sin\alpha = 0.5$. From Fig. 5, we see that the region corresponding to this set of parameters has no stable solutions. Under the conditions of this problem, $Q^2 = (kq^2)/(mgl^2) \approx 0.063$. Corresponding to these values of L and Q^2 is curve *1* in Fig. 4, whereas corresponding to the unstable equilibrium point found in the problem is the maximum at this point.

We note that the problem has a correct solution if posed differently. For example: "Given a charge of 20 nC, find the angular deviation of the string." From the dependence $W(x)$ (curve *1* in Fig. 4) for the parameters of the problem, it is possible to determine which minimum on the curve corresponds to the stable equilibrium position. The result is $x = \sin\alpha \approx 0.129$, and hence $\alpha \approx 7.4°$.

4. Nonlinear oscillations of the pendulum

We now consider the dynamics of an electrostatic pendulum, taking the friction force into account. The equation of motion of a physical pendulum is $I\ddot{\alpha} = \sum_i M_i$, where I is the moment of inertia of the pendulum about the axis of rotation, and M_i are the moments of the external forces acting on the pendulum. In our case, we can write

$$I\ddot{\alpha} = Fb\cos\alpha - mga\sin\alpha - \gamma\dot{\alpha}\,. \tag{13}$$

The last term in the right-hand side of Eqn (13) is the moment of inertia of the force of friction, which is proportional to the angular velocity. The Coulomb force acting on the ball from its image in the conducting plate is

$$F = \frac{kq^2}{4(L - b\sin\alpha)^2} = \frac{kq^2}{4b^2(\widetilde{L} - \sin\alpha)^2}\,, \quad \widetilde{L} = \frac{L}{b}\,. \tag{14}$$

(The tilde is dropped hereafter). We make the equation of motion dimensionless by dividing both sides by mga and choosing the time unit such that the coefficient of $\ddot{a}$ is unity: $[t] = \sqrt{I/(mga)}$. In its final form, the equation of the motion

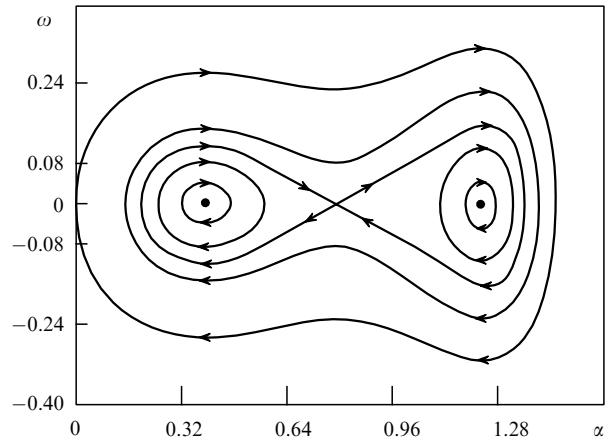

Figure 8. Phase portrait of an electrostatic pendulum with $L = 1.29$; $Q^2 = 0.34$.

of the pendulum becomes

$$\ddot{\alpha} + \beta\dot{\alpha} + \sin\alpha - \frac{Q^2\cos\alpha}{(L - \sin\alpha)^2} = 0\,,$$

$$Q^2 = \frac{kq^2}{4mgab}\,, \quad \beta = \frac{\gamma}{\sqrt{Igma}}\,. \tag{15}$$

Numerical integration of this equation using the MathCad package gave the following results.

Figure 8 shows the phase diagram of the physical electrostatic pendulum in the case where it forms a conservative system with $\beta = 0$ and $L = 1.29$; $Q^2 = 0.34$ (for all phase trajectories shown, $\dot{\alpha}(t = 0) = \omega(t = 0) = 0$). Corresponding to Fig 4 (curve *5*), the phase diagram features two centers (black dots), a saddle point corresponding to a local minimum, and separatrix branches passing through the saddle point.

The shape of oscillations and the phase trajectory resulting from the integration of Eqn (15) with the initial conditions $\alpha(t = 0) = \dot{\alpha}(t = 0) = 0$ are another example to consider. Of particular interest is the moderate charge, the $L > 1$ case, where the potential energy of the pendulum has two local minima. Figure 9 shows the time variation of the angular coordinate and the corresponding phase trajectory of the parameters $L = 1.25$, $Q^2 = 0.284$, and $\beta = 0.005$. It can be seen that oscillations initially cover almost the entire range of the angular coordinate and then concentrate around the stable focus at (0.31, 0).

5. Equilibrium, stability, and oscillations of a spring pendulum

We now consider the case of an electrostatic pendulum. Figure 10 illustrates the ways in which the problem can be formulated in this case (k is the rigidity of the spring, which is assumed to work in both tension and compression).

In the case shown in Fig. 10b, an image charge (shown dashed) forms on the grounded plate. We neglect the force of gravity as obviously of little or no importance. We also assume that at the initial instant, the spring is undeformed and that the balls instantly receive a charge q, and we let L denote the center-to-center distance between the upper and lower balls (in the case in Fig. 10b, L is the distance from the

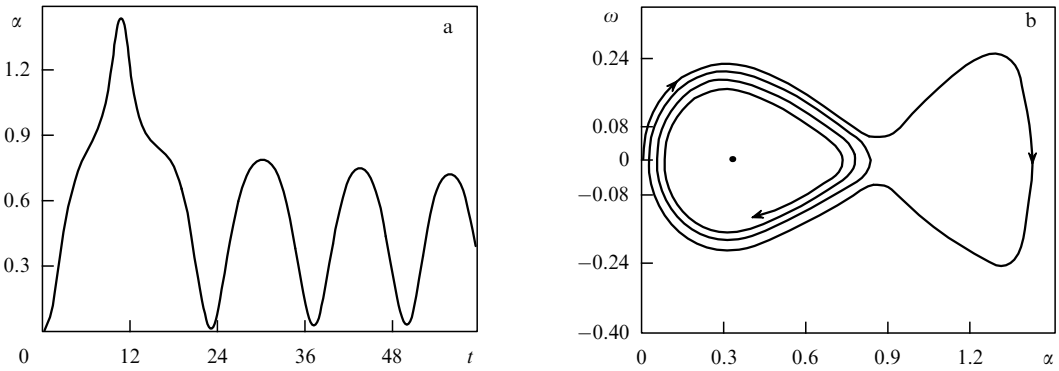

Figure 9. (a) Angular coordinate vs time and (b) the corresponding phase trajectories for the pendulum parameters $L = 1.25$, $Q^2 = 0.284$, and $\beta = 0.005$.

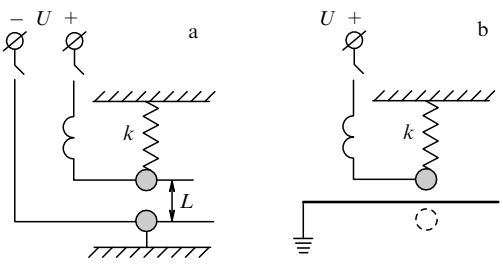

Figure 10. Schematic diagrams of electrostatic spring pendulums.

center of the ball to the plate). We consider the balls to be point-like charges for simplicity and concentrate in what follows on the situation shown in Fig. 10a. (Reference [12] was the first to address this problem.)

If no electrical breakdown occurs, then, when the voltage is switched on, the upper ball starts moving down. To see how it behaves further on, we write the potential energy it gains due to its displacement downward by x:

$$W = \frac{kx^2}{2} + k_e q^2 \left(\frac{1}{L} - \frac{1}{L-x} \right), \quad k_e \equiv \frac{1}{4\pi\varepsilon_0} . \tag{16}$$

The potential energy is taken to be zero at the initial position of the ball. Using the length L and the energy $kL^2/2$ to pass to dimensionless variables, we obtain the equation

$$W(x) = x^2 - Q^2 \frac{x}{1-x}, \quad Q^2 = \frac{2k_e q^2}{kL^3} . \tag{17}$$

Figure 11 shows the plot of $W(x)$ for different Q^2 (curves *1*, *2*, *3* are for $Q^2 = 0.15$, 0.23, 0.30). We see that starting from a certain value Q_*^2, the function $W(x)$ shows no local minima, which means that Q_*^2 is a bifurcation value of Q^2 that separates the region where the pendulum can have equilibrium positions (including a stable one) from the region where it cannot. To determine Q_*^2, we find the force acting on the ball and set it equal to zero to obtain

$$F_x = -2x + \frac{Q^2}{(1-x)^2} = 0, \quad \text{or} \quad Q^2 = 2x(1-x)^2 . \tag{18}$$

It is easily seen that the right-hand side of the last equality has a local maximum at $x_m = 1/3$. The maximum value $Q^2(x_m)$, which is exactly the one corresponding to Q_*^2, is

$$Q_*^2 = \frac{8}{27} \approx 0.296 . \tag{19}$$

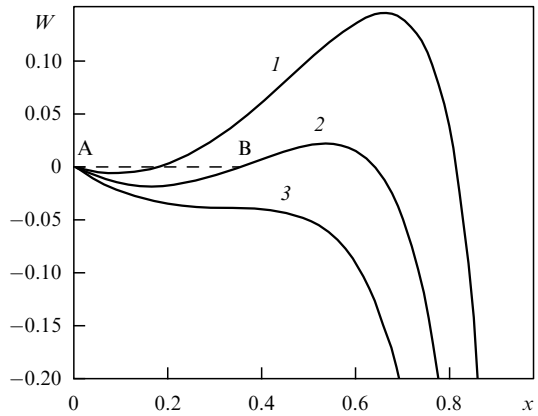

Figure 11. Potential energy of the spring pendulum vs displacement in dimensional units. Curves *1*, *2*, *3* are for $Q^2 = 0.15$, 0,23, 0.30.

(Interestingly, $Q_* = (2/3)^{3/2}$.) For $Q^2 < Q_*^2$, Eqn (18) has two real roots in the interval $0 \leqslant x \leqslant 1$, of which the smaller (greater) corresponds to the stable (unstable) equilibrium position.

There are therefore two types of motion possible for the upper ball: it can either undergo damped oscillations near the bottom of the potential well (which is a stable equilibrium position) or monotonically approach the second ball to within an arbitrarily small neighborhood, depending on whether the parameters of the problem are such that $Q^2 < Q_*^2$ or $Q^2 \geqslant Q_*^2$. Another point to note is this. If the system is nearly frictionless, then, in the case where the potential energy has a local maximum below line AB in Fig. 11, the upper ball starting its motion from point A can pass the local maximum position and undergo a transition to a state in which it irreversibly moves toward the lower ball. The critical value of Q^2 at which this occurs is found by requiring $W(x) = W(x = 0) = 0$, giving

$$x^2 - \frac{Q^2}{1-x} + Q^2 = 0 . \tag{20}$$

Noting that x should also satisfy the maximum condition for the potential energy, Eqn (18), and eliminating Q^2 from Eqn (20), we obtain $x_m = 1/2$. The corresponding critical value is $Q_1^2 = 1/4 = 0.25$.

The following magnetic analogy of the problem discussed here is well known [13]. A lead of length l with a current I_1 is

suspended by two springs of rigidity k. Placed at a distance L from the lead, in the same plane, is another, infinite-length lead though which a current I_2 is passed at the initial instant. The motion of the short-length lead and its possible equilibrium positions are here determined by the parameter $J^2 = \mu_0 I_1 I_2 l/(4\pi k L^2)$ (an analog of Q^2). The bifurcation value of J^2 separating regions with and without a stable equilibrium point is $J_*^2 = 1/4$.

Thus, it follows from the above that the problem of the motion of the electrostatic pendulum is analogous, but not identical, to that of the magnetic spring pendulum. Indeed, there is an essential difference between them in that in the former case, an electrical breakdown inevitably occurs in the air gap between the oppositely charged balls as they approach each other arbitrarily close.

6. Self-oscillations

It is shown, for example, in Ref. [12] that as two oppositely charged balls approach each other more closely, the field in the air gap between them infinitely increases in strength, which means, for the situation in Fig. 10a, that the gap is inevitably broken down electrically for $Q^2 \geqslant Q_*^2$. Now, if the two balls acquire the initial charges at the instant when the upper ball returns to its initial position, the process repeats itself. We thus conclude that for the appropriate parameter values for the electrical circuit in Fig. 12a, it can be successfully used to induce self-oscillations in the system.

Such self-excited systems, referred to as electromechanical, are well known and classically exemplified by a spring pendulum carrying an electrical current (see, e.g., Ref. [14]). The spring of this pendulum has its end immersed in a conducting liquid. When a current is passed through the spring, Ampere forces act to contract it, the current ceases to flow, and the spring moves downward under the action of gravity, causing the entire process to repeat.

Due to their self-excitation mechanism, such oscillations are called discontinuous (relaxation) oscillations [13–16], one example being capacitor voltage oscillations. Discontinuous oscillations involving an electrical discharge arise in the circuit shown in Fig. 12b, with neon lamp N acting as a discharger [13, 15], although a simpler alternative featuring an air gap between electrodes is also a possibility [16].

The major difference between the circuits in Fig. 12a and Fig. 12b is that the former has its oscillation period determined by the relaxation time $\tau = RC$, whereas the latter, by the natural oscillation period $T = 2\pi\sqrt{m/k}$, with m being the mass of the ball. In this case, implementing positive feedback requires that the relaxation time be close to half the natural oscillation period, $RC \approx T/2$ (assuming that the discharge time is negligibly small). We note that the condition $Q^2 \geqslant Q_*^2$ is not necessary for the system in Fig. 12a to develop self-oscillations because, if gap breakdown occurs within the interval AB in Fig. 11, self-oscillation are also possible, even if smaller in amplitude. Because the event in which equilibrium loses its stability is critical by its nature, the self-oscillations within the interval AP can be called precritical, and those at $Q^2 \geqslant Q_*^2$, postcritical. Reference [12] describes our experiments on precritical oscillations of a spring-suspended steel ball.

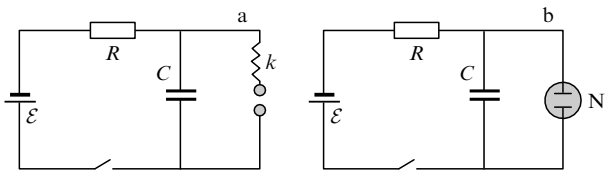

Figure 12. Circuits implementing discontinuous self-oscillations. N is a neon lamp.

It is inevitable that electromechanical systems are subject to friction. The way friction affects self-oscillations can be understood by numerically simulating how such oscillations develop in the system shown in Fig. 10a. Introducing a friction force proportional to the velocity, we can write the equation of motion of the upper ball as

$$m\ddot{x} = -kx - \gamma\dot{x} + \frac{k_e q^2}{(L-x)^2}\,, \tag{21}$$

where m is the ball mass and γ is the friction coefficient. To reduce the number of parameters, we use the length scale L and time scale $\sqrt{m/k}$ to pass to dimensionless variables, which yields

$$\dot{v} = -x - \beta v + \frac{Q^2}{2(1-x)^2}\,, \quad \dot{x} = v\,, \quad \beta = \frac{\gamma}{k}\,. \tag{22}$$

This system of two first-order differential equations was integrated numerically with the initial conditions $x(t=0) = v(t=0) = 0$ assuming, for simplicity, that the charging and discharging of the balls are instantaneous processes. For $Q^2 = 0.23$ and $t = 0$ (the first case considered), integration shows that immediately after the condition $x > 0.3$ is satisfied, both balls have their charge instantaneously reduced to zero ($Q^2 = 0$ at $x > 0.3$) and that they immediately regain their initial charge $Q^2 = 0.23$ when the upper ball moves upwards, even for $x < \delta$. Calculations were mainly performed for $\delta = 0.001$. Therefore, Eqns (22) must be solved with the conditions

$$Q^2 = 0.23 \text{ at } t = 0\,, \quad Q^2 = 0 \text{ if } x > 0.3 \text{ and } \dot{x} > 0\,,$$
$$Q^2 = 0.23 \text{ if } x < \delta \text{ and } \dot{x} < 0\,. \tag{23}$$

Figure 13 shows the results of the integration of system (22) with conditions (23) for $\beta = 0.05$ (curve *1*) and $\beta = 0.15$ (curve *2*). Oscillations set in in the interval $-0.487 < x < 0.599$ for the friction coefficient $\beta = 0.05$ and in the interval $-0.240 < x < 0.394$ for $\beta = 0.15$, within about ten or four

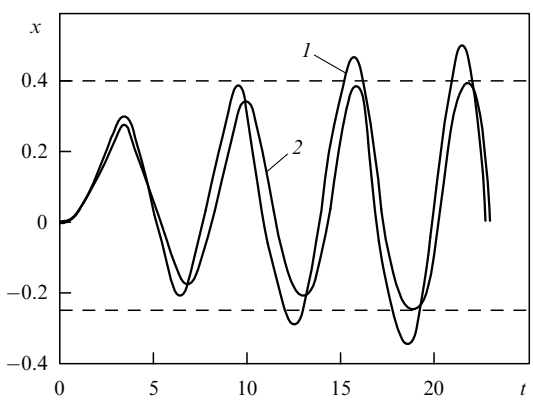

Figure 13. Time dependence of the ball center coordinate, illustrating how the self-oscillations of the electrostatic spring pendulum set in for $\beta = 0.05$ (curve *1*) and $\beta = 0.15$ (curve *2*).

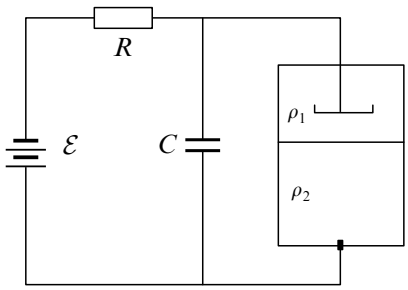

Figure 14. Schematic setup for the observation of the self-oscillations of a liquid–liquid interface in an external electrical field.

oscillation periods, respectively (the setting-in criterion is that increasing the calculation accuracy leaves the minimum or maximum value of x unchanged to within three significant digits; the corresponding limits are shown dashed). It can be seen that increasing friction decreases both the swing of the oscillations and the time it takes for them to set in.

As expected, the oscillations have a period close to that of the natural oscillations of the spring, i.e., $T \approx 2\pi$ in the units chosen. A change of ± 0.01 in the coordinate δ close to which the balls regain their previous charge indicates that the oscillation amplitude slightly increases as δ increases and decreases when it decreases.

Integrating system (22) with conditions (23) for $Q^2 = 0.4$ (postcritical state) and with all other parameters unchanged left the main conclusions unaltered. The oscillation amplitude increased and was found to be $(-0.628, 0.798)$ for $\beta = 0.05$ and $(-0.300, 0.523)$ for $\beta = 0.15$.

Self-oscillations of an electrostatic spring pendulum are analogous to those occurring in distributed oscillatory systems with a continuous set of frequencies. An example is the oscillations of a liquid–liquid interface in an external electric field. These were observed in Ref. [17] using the setup (see Fig. 14) consisting of a cylinder that contains a solution of table salt (NaCl, density ρ_2) and a layer of kerosene (density ρ_1). Other setup parameters were as follows: resistance, $R = 10$ mΩ, capacitor capacitance $C = 100-400$ pF, and a smoothly time-varying voltage from a high-voltage source, up to 15 kV. In kerosene, at a distance of 1.5–2.0 cm from the interface between the two liquids, was one electrode, the second one being the interface. Increasing the voltage to a certain critical value (of the order of 7 kV) makes the equilibrium of the flat interface unstable, with the result that gravitational capillary waves of peaks and troughs develop on the surface: a phenomenon well known as the Tonks–Frenkel instability (see, e.g., Ref. [12]). This instability leads to the breakdown of the kerosene layer and, ultimately, only one fundamental mode, with a wavelength of about 2/3 the cylinder diameter, takes part in the breakdown and in the oscillations that set in. The self-oscillations are in this case postcritical, because they occur after the system has lost its stability.

Capillary oscillations can also occur on the surface of a single liquid droplet, such that under certain conditions, a droplet of a conducting liquid can also participate in discontinuous self-oscillations. Experimenter A I Zhakin, who serendipitously observed such oscillations, kindly provided us with some results, including a video. The video snapshots in Fig. 15 feature a liquid droplet oscillating in an external electric field at the end of a capillary and show the three successive phases it passes through. The liquid was water, the potential difference between the capillary and the electrode (a ring 0.5 cm in radius made of wire 2 mm in diameter and placed 2 cm above the capillary end) was about 5 kV, the diameter of the capillary was 1 mm. The time interval between the neighboring phases shown in Fig. 15 corresponds to a quarter of the oscillation period and equals 0.13 s, and the oscillation period of the droplet is correspondingly 0.52 s (oscillation frequency $\omega = 12$ s^{-1}). It is seen that the phase in Fig. 15b is one in which the droplet stretches in length and loses its charge (the latter fact giving rise to a violet glow). Because the frequency spectrum of the capillary oscillations of the droplet depends on the charge on the drop and the strength of the external field [12], the $n = 2$ fundamental mode may well have an oscillation frequency about 12 s^{-1}.

We note that the corona discharge is not the only reason why the droplet can lose its charge: the same can occur if the equilibrium ellipsoidal shape of the droplet surface becomes unstable [12]. The condition for this is arguably that the electrical pressure on the surface of the droplet exceeds the Laplace pressure,

$$\frac{\varepsilon_0 E^2}{2} > \frac{2\sigma}{R}\,, \tag{24}$$

where σ is the surface tension coefficient of water, E is the electric field strength on the droplet surface, and R is the curvature radius of this surface. With $r = 0.5$ mm and $\sigma = 72$ mN m^{-1}, Eqn (24) yields the field strength estimate $E > 80$ kV cm^{-1}. Because such a value was hardly achievable in the experiments reviewed, it is to be concluded that a corona discharge was underlying the loss of charge, and the self-oscillations were therefore precritical. We note in conclusion that the conditions of the experiments above can well be reproduced — and hence a similar phenomenon can also occur — in natural environments (in a thunderstorm, for example).

Figure 15. Photographs of three successive phases of an oscillating droplet in an external electric field.

7. Conclusions

The experiments performed to measure the force exerted on a charged ball by its image in a grounded conducting plate showed that from the standpoint of formation of the electrical image, a large grounded plate is equivalent to a conducting half-space: the electrical image in the plate turns out to be full, $q' = -q$, and the force obeys the Coulomb law and is equal to $F = kq^2/4S^2$, where S is the distance from the center of the ball to the plate. Moreover, there is an interesting property the electrostatic pendulum exhibits in this situation as a key element of the electrostatic dynamometer: for the same set of parameters, the pendulum can have two equilibrium positions and one nonequilibrium position.

An examination was performed, both theoretically and experimentally, of the ways in which a ball can interact with a conducting plate. There are two key (control) parameters in such a system, one proportional to the square of the charge of the ball and the other to the original distance between the ball and the plate. Plotted in the plane of these parameters was a bifurcation line separating the region of parameters in which the pendulum has stable equilibria from the region where it does not. In the (Q^2, x) plane, stable and unstable states are mapped and experimental points are shown where one or two stable equilibria were observed. It is pointed out that some undergraduate exercise books [9–11] give an incorrect formulation of the problem of the equilibrium of an electrostatic pendulum by overlooking the fact that some pendulum positions (found as solutions) can be unstable.

By numerically solving the equation of motion of the physical electrostatic pendulum, its nonlinear oscillations are considered and its phase portrait is constructed.

Also, the dynamics of the electrostatic spring pendulum are examined. It is shown that this system, with one control parameter Q^2 proportional to the square of the charge of the balls, has a bifurcation point that separates the region where stable states exist from the region where they do not. In the case where a system of a spring pendulum can have an electric charge and the balls are connected to a DC voltage source, it is found that self-oscillations at a near-natural frequency are possible. Examples are given of distributed capillary electrostatic oscillators (that is, of those characterized by a continuous set of natural frequencies) with self-oscillations occurring at the fundamental mode frequency.

Acknowledgements. A B Fedorov's assistance in conducting the experiments is appreciated.

References

1. Saranin V A, Mayer V V *Usp. Fiz. Nauk* **180** 1109 (2010) [*Phys. Usp.* **53** 1067 (2010)]
2. Bugaevskii M Yu, Ponomarenko V I *Issledovanie Povedeniya Tsepi Chua* (Research into the Behavior of the Chua Circuit) (Saratov: Kolledzh, 1999)
3. Matsumoto T A *IEEE Trans. Circuits* **31** 1055 (1984)
4. Nikitina N V, Repots of the National Academy of Sciences of Ukraine No. 12 (2007)
5. Landau L D, Lifshitz E M, Pitaevskii L P *Elektrodinamika Sploshnykh Sred* (Electrodynamics of Continuous Media) (Moscow: Nauka, 1982) [Translated into English (Oxford: Pergamon Press, 1984)]
6. Batygin V V, Toptygin I N *Sbornik Zadach po Elekrodinamike* (Problems in Electrodynamics) (Moscow: Nauka, 1970) [Translated into English (London: Academic Press, 1978)]
7. Vekshtein E G *Sbornik Zadach po Elektrodinamike* (Electrodynamics Problem Solving Book) (Moscow: Vysshaya Shkola, 1966)
8. Saranin V A *Usp. Fiz. Nauk* **169** 453 (1999) [*Phys. Usp.* **42** 385 (1999)]
9. Chertov A G, Vorob'ev A A *Zadachnik po Fizike* (Physics Problem Solving Book) (Moscow: Vysshaya Shkola, 2009)
10. Ruban I I et al. *Fizika: Zadaniya k Prakticheskim Zanyatiyam* (Practical Physics Assignments) (Minsk: Vysheishaya Shkola, 1989)
11. Aliev I N, Tolmachev V V *Sbornik Zadach po Elektrodinamike* (Electrodynamics Problem Solving Book) (Moscow: Izd. MGTU im. N E Baumana, 1996)
12. Saranin V A *Ustoichivost' Ravnovesiya, Zaryadka, Konvektsiya i Vzaimodeistvie Zhidkikh Mass v Elektricheskikh Polyakh* (Stable Equlibrium, Charging, Convection and Interaction of Liquid Masses in Electric Fields) (Moscow – Izhevsk: RKhD, 2009)
13. Andronov A A, Vitt A A, Khaikin S E *Teoriya Kolebanii* (Theory of Oscillators) (Moscow: Nauka, 1981) [Translated into English (Oxford: Pergamon Press, 1966)]
14. Malov N N *Osnovy Teorii Kolebanii* (Basic Theory of Oscillations) (Moscow: Prosveshchenie, 1971)
15. Kharkevich A A *Avtokolebaniya* (Self-Excited Oscillations) (Moscow: Gostekhizdat, 1953)
16. Teodorchik K F *Avtokolebatel'nye Sistemy* (Self-Excited Oscillation Systems) (Moscow – Leningrad; OGIZ, Gostekhizdat, 1948)
17. Nesterov S V, Sekerzh-Zen'kovich S Ya *Dokl. Akad. Nauk SSSR* **256** 318 (1981) [*Sov. Phys. Dokl.* **26** 20 (1981)]